Biochemistry and Biophysics Reports 32 (2022) 101389

Contents lists available at ScienceDirect

Biochemistry and Biophysics Reports

journal homepage: www.elsevier.com/locate/bbrep

Prognostic pyroptosis-related lncRNA signature predicts the efficacy of immunotherapy in hepatocellular carcinoma

Zina Cheng [a], Juechen Han [a], Fa Jiang [a], Weiyi Chen [a], Xiaolu Ma [a,b,*]

[a] College of Biomedical Engineering, Taiyuan University of Technology, Taiyuan, 030024, China
[b] State Key Laboratory of Membrane Biology, Institute of Zoology, University of Chinese Academy of Sciences, Chinese Academy of Sciences, Beijing, 100101, China

ARTICLE INFO

Keywords:
Hepatocellular carcinoma
Long non-coding RNA
Pyroptosis
Immunotherapy

ABSTRACT

Hepatocellular carcinoma (HCC), a common malignant tumor of the liver, remains high incidence and poor prognosis. Although pyroptosis as well as lncRNA have been believed to play important roles in the tumorigenesis, diagnosis and prognosis, the role of pyroptosis-related lncRNAs (PRlncRs) in HCC remains obscure. Here, we identified 73 significantly differentially expressed and overall survival (OS) related pyroptosis-related lncRNAs (PRlncRs) in noncancerous and HCC samples. Based on LASSO regression and Cox regression analyses, we set up a novel prognostic model including six PRlncRs (MKLN1-AS, AC139491.2, AC145207.5, AC099850.3, AL590705.3 and AL049840.5), which showed good correlation with the OS of HCC patients. Considering that the risk score was negatively related to clinicopathologic features including T stage (T1-2 and T3-4), clinical stage (stage I-II and stage III-IV) and histological grade (G1, G2, G3 and G4), we further constructed a predictive nomogram containing the risk score and other clinicopathological features to predict the OS rates for HCC patients. In addition, the proposed signature was closely related to immune infiltration and offered improved clinical utility for immune checkpoint inhibitors (ICIs) strategies and chemotherapeutic drug selection in HCC. In conclusion, we established a considerable accurate risk signature consisting of 6 PRlncRs in HCC, which could predict the prognosis and efficacy of immunotherapy for HCC patients.

Author statement

Xiaolu Ma and Weiyi Chen conceived the study. Zina Cheng and Juechen Han analyzed the data based on TCGA LIHC cohort. Zina Cheng and Fa Jiang performed the validation of external dataset and analyzed the calibration curves. Xiaolu Ma, Juechen Han and Zina Cheng wrote the manuscript. All authors read and approved the manuscript for publication.

1. Introduction

Hepatocellular carcinoma (HCC) is the most prevalent primary hepatic malignancy worldwide, with high incidence and mortality rates, as well as poor prognosis [[1,2]]. Recently, both of inflammation and aberrant hepatocyte death were considered to be tightly associated with HCC progression. Besides traditional surgical resection and chemoradiotherapy, immunotherapy especially immune checkpoint inhibitors (ICIs) has made great progress in HCC treatment, offering hope of improving the prognosis of HCC patients [3]. However there remains a critical issue to precisely identify the population of HCC patients that can benefit from immunotherapy, while the overall objective response rate of ICI fall within 20% [4]. Therefore, uncovering novel biomarkers for the prognosis of HCC would be of urgent need and great significance.

Pyroptosis, a newly observed cellular inflammatory necrosis, is mediated by gasdermin (GSDM) which is stimulated by inflammasomes [5]. Recently, emerging studies have demonstrated that pyroptosis plays a critical role in tumorigenesis and cancer therapy [6]. For example, anticancer drugs such as metformin [7], anthocyanins [8], docosahexaenoic acid (DHA) [9] and dipeptidyl peptidase 8 and 9 (DPP 8/9) [10] could lead to tumor pyroptosis. Pyroptosis has been shown to be important in HCC progression, making pyroptosis a potential treatment target for HCC. Long noncoding RNA (lncRNA) which is longer than 200 nucleotides with low protein coding potential, plays an important role in the proliferation, invasion and metastasis of tumor cell [[11,12]]. Particularly, lncRNAs such as HAND2-AS1, PCNAP1 and HOXD-AS1, have been reported to be biomarkers for the diagnosis and prognosis of HCC [[13–15]]. While the relationship between pyroptosis-related genes (PRGs) and the prognosis of ovarian cancer and lung

* Corresponding author. College of Biomedical Engineering, Taiyuan University of Technology, Taiyuan, 030024, China.
E-mail address: maxiaolu@tyut.edu.cn (X. Ma).

https://doi.org/10.1016/j.bbrep.2022.101389
Received 13 July 2022; Received in revised form 8 November 2022; Accepted 14 November 2022

adenocarcinoma (LUAD) has been identified [[16–18]], it is still obscure about the role of pyroptosis-related lncRNAs in prognosis prediction of HCC.

In this study, we identified 6 differentially expressed pyroptosis-related lncRNAs (PRlncRs) in HCC patients and constructed a novel risk signature for the prognosis and efficacy of ICI treatment prediction, providing new perspectives for prognostic biomarkers for HCC.

2. Materials and methods

2.1. Data acquisition

The RNA-seq data and corresponding clinical information were downloaded from the liver hepatocellular carcinoma (LIHC) cohort of TCGA (https://portal.gdc.cancer.gov/repository), including 50 noncancerous and 374 HCC samples. The pyroptosis-related genes sets include 27 pyroptosis-related genes from M41805 gene set (https://www.gsea-msigdb.org/gsea/msigdb) (Table S1) and 33 pyroptosis-related genes from relevant literature [19] (Table S2). Moreover, the RNA-seq data and clinical information of 148 HCC patients from GSE141198 using GEO database (http://www.ncbi.nlm.nih.gov/geo) were used as external validation.

2.2. Differential expressed PRlncRs identification

Based on Pearson correlation, we analyzed the association between PRGs and lncRNA (|Pearson correlation coefficient| > 0.4, $p < 0.001$). Next, we selected differentially expressed PRlncRs using "limma" package of R software (|$\log_2$FC| > 1, $p < 0.05$).

2.3. PRlncR signature construction and validation

First, we identified candidate prognostic lncRNAs from the training set using the univariate Cox regression at the threshold of $p = 0.05$. Next, we performed LASSO regression using a 10 fold cross-validation and $p = 0.05$ threshold to reduce overfitting lncRNAs. Lastly, we constructed a prognostic PRlncR signature via multivariate Cox regression: risk score = level lncRNA 1 × coefficient 1 + level lncRNA 2 × coefficient 2 + level lncRNA 3 × coefficient 3 + … … + level lncRNA n × coefficient n. According to the median value of risk score, HCC patients were divided into high- and low-risk groups and the OS time was calculated between these two subgroups by Kaplan-Meier analysis. The predictive accuracy of the risk score was measured by performing time receiver-operating characteristic (ROC) analysis. Combined with clinical characteristics, risk scores were further utilized to develop a predictive nomogram to predict the 1-, 2- and 3-year OS for HCC patients.

2.4. PCA and t-SNE analysis

Principal component analysis (PCA) and *t*-distributed stochastic neighbour embedding (*t*-SNE) were carried out for dimensionality reduction analysis and assessing the clustering ability of the predictive model for HCC patients using the "Rtsne" and "ggplot2" R packages.

2.5. Chemotherapeutic response analysis

The half-maximal inhibitory concentration (IC50) to Axitinib and Sorafenib between high- and low-risk HCC patients were analyzed using "limma" package in R based on the pRRophetic package.

2.6. Immune infiltration analysis

The infiltration situation of immune cells between high- and low-risk groups using the CIBERSORT algorithm. The threshold value was set as $p = 0.05$.

2.7. Predicting a patient' s response to ICI therapy

The scores of immune signal pathways were analyzed by single-sample gene set enrichment analysis (ssGSEA). The TMB scores of HCC patients were analyzed using the maftools package. The scores of MSI were calculated from the Tumor Immune Dysfunction and Exclusion (TIDE) website (http://tide.dfci.harvard.edu/). The scores of IPS were extracted from The Cancer Immunome Atlas (TCIA). The values of TMB and MSI, and the gene expression levels of PD-L1, PD-1 and CTLA4 were compared using "limma" package of R software.

2.8. Statistical analysis

All statistical analysis were performed by R software (4.0.3). Analysis of the differences between the high- and low-risk cohorts was accessed by Student's *t*-test and Chi square test. $P < 0.05$ was considered as statistically significant.

3. Results

3.1. Identification of differentially expressed PRlncRs in HCC

Through literature review and data retrieval, we first obtained 52 pyroptosis-related genes (PRGs) (Table S3). Based on the 52 PRGs, we identified 764 pyroptosis-related lncRNAs (PRlncRs) in the TCGA LIHC cohort by Pearson correlation analysis (Table S4). Next, via comparing the expression levels of 764 PRlncRs in both 50 noncancerous and 374 HCC samples, we identified 524 significantly differentially expressed pyroptosis-related lncRNAs (PRlncRs) (Table S5), comprising 518 upregulated and 6 downregulated PRlncRs.

3.2. Establishment of a PRlncR model

To construct a prognostic PRlncR model, we first classified the included cases (n = 365) into training (n = 245) and validation (n = 120) sets at 2:1 ratio randomly. To check the prognostic value of the 524 differentially expressed PRlncRs, we performed a univariate Cox regression analysis using the "survival" R package. As is shown, 73 PRlncRs were meaningfully correlated to the overall survival (OS) in the training set. To avoid overfitting, we further utilized the "glmnet" R package to conduct LASSO regression analysis and discovered 11 PRlncRs predicting the HCC prognosis (Fig. 1A–B). Based on the training set, we performed a multivariate Cox proportionate perils regression analysis and established a prognostic PRlncR risk model including 6 lncRNAs (MKLN1-AS, AC139491.2, AC145207.5, AC099850.3, AL590705.3 and AL049840.5). The risk score = (0.87992 × MKLN1-AS) + (0.51858 × AC139491.2) + (0.44334 × AC145207.5) + (0.06734 × AC099850.3) + (0.79013 × AL590705.3) + (0.07392 × AL049840.5) (Fig. 1C and Fig. S1A). Moreover, we discovered mRNAs related to the 6 PRlncRs (Fig. 1D) and performed gene set enrichment analysis (GSEA) to detect possible biological signaling pathways related to HCC patients. As is shown, complement and ubiquitin mediated proteolysis ($p < 0.001$), spliceosome ($p < 0.001$), RNA degradation ($p < 0.001$), oocyte meiosis ($p < 0.001$) and nucleotide excision repair ($p < 0.001$) pathways were significantly stimulated in high-risk patients (Figs. S1B–F and Table S6). Whereas complement and coagulation cascades ($p < 0.001$), retinol metabolism ($p < 0.001$), glycine, serine and threonine metabolism ($p < 0.001$), fatty acid metabolism ($p < 0.001$) and drug metabolism cytochrome P450 ($p < 0.001$) pathways were activated in low-risk HCC patients (Figs. S1G–K and Table S6).

Based on the risk score, we divided these HCC patients into high- and low-risk groups and verified the predictive performance of the 6 PRlncRs prognostic model. As is shown, the Kaplan-Meier survival curves evaluated via the "survminer" and "pROC" R package showed that HCC patients with high-risk scores (13.87 months) had a worse OS probability than those with low-risk scores (21.83 months) ($p < 0.001$, Fig. 2A,

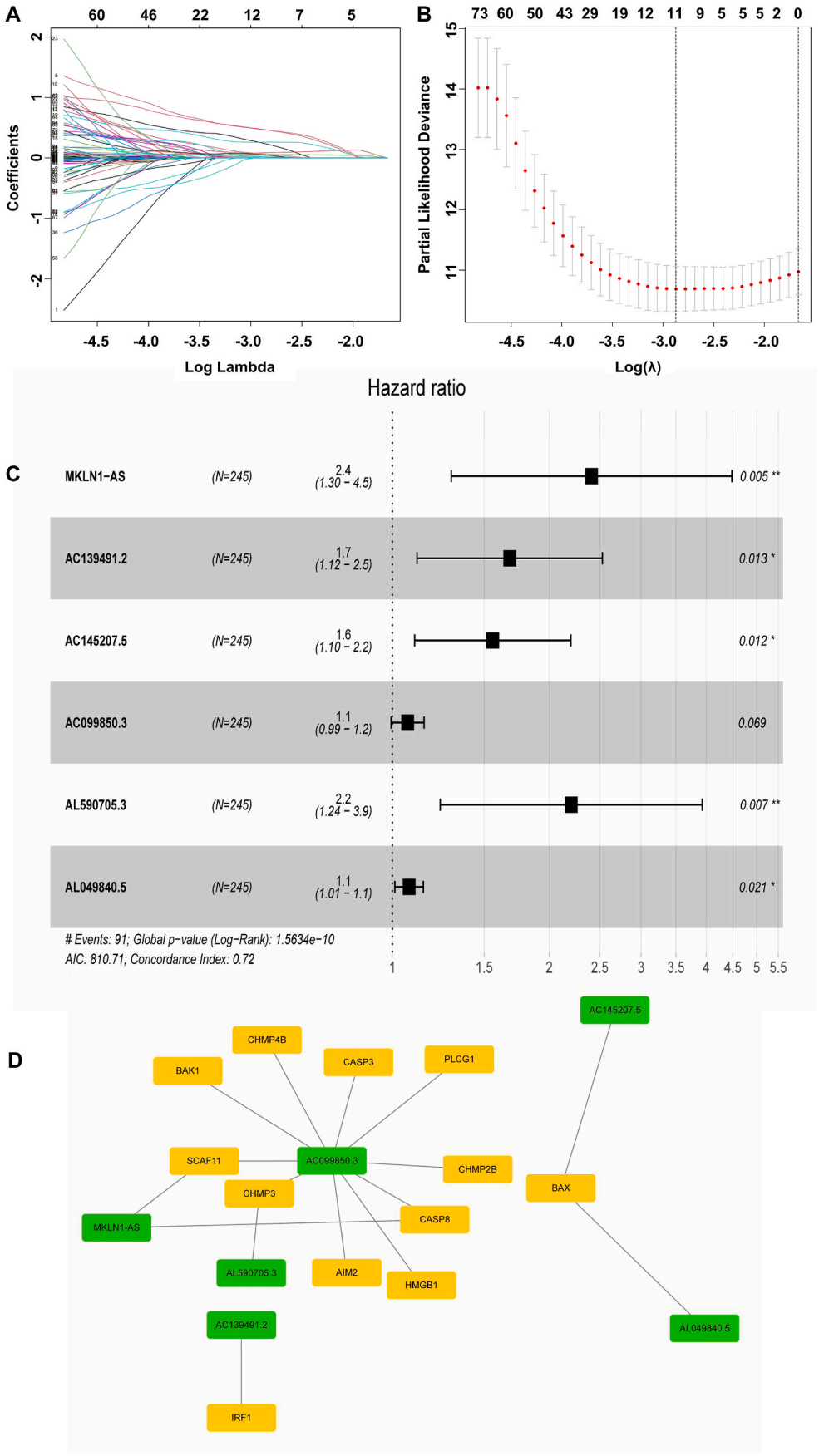

Fig. 1. Construction of prognostic PRlncRs model. (A) Forest plot of 73 prognostic PRlncRs. (**B**) Correlation plot of 73 PRlncRs with survival prognostic value. (**C**) Hazard ratio for the pyroptosis-related prognostic signature containing 6 lncRNAs. (**D**) Prognostic co-expression network of the 6 PRlncRs and mRNAs in HCC.

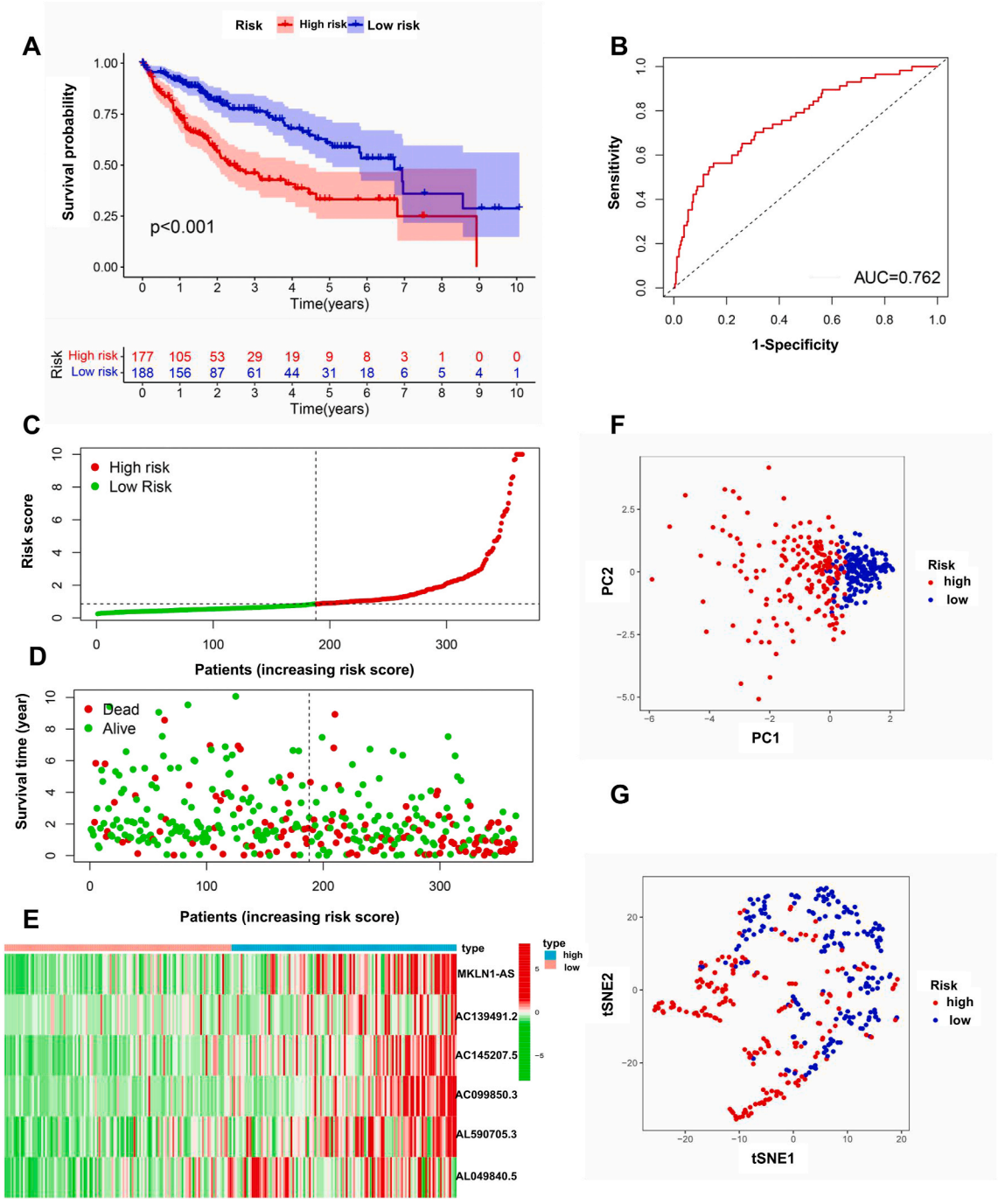

Fig. 2. Prediction of OS for HCC patients by the 6 PRlncR signature. (**A**) OS curves for HCC patients in the high- and low-risk group. (**B**) ROC curve of measuring the predictive value. (**C**) Distribution of risk score of patients with HCC. (**D**) Distribution of survival status for HCC patients. (**E**) Distribution of the expression profiles of 6 PRlncRs. (**F**) Principal components analysis (PCA) plot of the survival models in high- and low-risk groups. (**G**) *t*-SNE plot of the survival models in high- and low-risk groups.

Figs. S2A–B), with AUCs of 0.762, 0.787 and 0.711 in ROC curves respectively (Fig. 2B and Figs. S2C–D). To further determine the reproducibility of the risk score signature, we performed external validation based on a GEO dataset (GSE141198) including 148 HCC patients. Excitingly, consistent with the results from the TCGA LIHC cohort, the Kaplan-Meier curves revealed that the OS of HCC cases in the high-risk group was significantly lower than those in the low-risk group ($p = 0.038$), with AUC of 0.617 (Figs. S2E–F). In addition, along with the risk score increased, the risk of death increased and the survival time decreased (Fig. 2C–E and Fig. S3). Furthermore, we found that both PCA and *t*-SNE dimensionality reduction analysis could classify HCC patients into high-and low-risk clusters successfully (Fig. 2F–G). Together, these results demonstrated that our 6 PRlncRs prognostic model was of great confidence to predict the OS of HCC.

3.3. Construction of a predictive nomogram

To combine the clinicopathologic features and 6 PRlncRs prognostic model, we built a predictive nomogram through the "DynNom" R package and predicted the prognosis of HCC patients using univariate and multivariate Cox regression analyses. As a result, the risk score ($p < 0.001$) and clinical stage ($p < 0.001$) were independent prognostic

factors for HCC patients (Fig. 3A–B). Then, we separated the clinical features into subgroups including N stage (N0 and N1), M stage (M0 and M1), T stage (T1-2 and T3-4), clinical stage (stage I-II and stage III-IV), histological grade (G1, G2, G3 and G4), gender (male and female) and age (< = 65 and > 65) and found that T stage, clinical stage and histological grade were significant different between high- and low-risk groups via Chi-square test (Fig. 3C). Furthermore, we compared the risk scores in subgroups with different clinicopathological features and found that T stage, clinical stage and histological grade were positively related to the risk score, consisting with that the HCC patients with advanced clinical stage and higher histological grade tend to have poorer OS rate (Fig. 3D–F). Notably, ROC curves showed that 6 PRlncRs prognostic model was significantly better than clinical features such as age, gender, histological grade and clinical stage in the prognosis of HCC patients with AUCs of 0.761, 0.531, 0.509, 0.499 and 0.671 respectively (Fig. 3G). Besides, the calibration curves of constructed nomogram for the 1-, 2-, and 3-year OS showed good predictive ability in the entire cohort (Fig. S4). Therefore, we developed a novel nomogram containing the risk score and other clinicopathological features, which could be used as clinical adjuvant treatment management in the prediction of the prognosis for HCC patients (Fig. 3H).

3.4. PRlncRs were associated with drug sensitivity, tumor immune infiltration and ICI response in HCC

Based on the TCGA LIHC dataset, we investigated the association the risk score and the efficacy of chemotherapeutic drugs in HCC patients. As is shown, the low-risk group exhibited a higher drug sensitivity for both Axitinib ($p < 0.001$) and Sorafenib ($p = 0.00076$) (Fig. 4A–B) than the high-risk group, suggesting that HCC patients with low risk score would be more sensitive to Axitinib and Sorafenib. Given that pyroptosis is closely related to the tumor immune microenvironment, we wonder the correlation between 6 PRlncRs and immune infiltration. Based on the CIBERSORT algorithm, we first analyzed the infiltrate characteristics of immune cells in HCC. As is shown, the risk score was negatively correlated with abundance of $CD8^+$ T cells ($p=0.004$), memory activated $CD4^+$ T cells ($p < 0.001$), follicular helper T cells ($p < 0.001$), M1 macrophages cells ($p=0.003$) and positively associated with the immune infiltration levels of monocytes ($p < 0.001$), M2 macrophages cells ($p < 0.001$), eosinophils ($p = 0.027$) and neutrophils ($p < 0.001$) (Fig. 4C and Fig. S5A), suggesting that the 6 PRlncRs were significantly correlated with tumor immune infiltration in HCC. Consistently, HCC patients with higher infiltration level of $CD8^+$ T cells showed improved OS, while those with higher abundance of M2 macrophages cells exhibited poorer OS (Fig. 4D–E).

Next, we explored whether the 6 PRlncRs prognostic model could be utilized for the predication of immunotherapy. Using single-sample gene set enrichment analysis (ssGSEA), we compared the activities of 13 different immune-related signal pathways in HCC using the R package "GSVA". Antigen-presenting cell (APC) costimulation ($p < 0.001$), chemokine receptor (CCR, $p < 0.001$), checkpoint ($p < 0.001$), human leukocyte antigen (HLA, $p < 0.05$), major histocompatibility complex (MHC) class I ($p < 0.001$), parainflammation ($p < 0.001$), T cell coinhibition ($p < 0.05$) and T cell costimulation ($p < 0.001$) pathways were significantly enriched in high-risk HCC group, whereas type II interferon (IFN) response ($p < 0.001$) pathway was obviously down-regulated. (Fig. 4F). Considering the contribution of tumor mutation burden (TMB) and microsatellite instability (MSI) to ICI efficacy [20], TMB and MSI are commonly used as biomarkers for predicting response to immunotherapy. As is shown, there was no difference of TMB between patients with high or low risk scores (Fig. S5B). Notably, the risk signature was negatively related to MSI ($p < 0.001$) (Fig. S5C), hinting a correlation between the 6 PRlncRs and ICI response. To prove it, we calculated immunophenoscore (IPS) scores of PD-1 and CTLA4 for HCC. Encouragingly, both the scores of IPS-PD1 and IPS-CTLA4 in low-risk group were distinct higher than those in high-risk HCC patients ($p = 0.024$ and $p = 0.0065$, respectively) (Fig. 4G–H), indicating that HCC patients with low risk score might benefit from ICI treatment. Moreover, we compared the expression levels of immune checkpoints and found that there was no significant changes of intratumoural programmed death ligand 1 (PD-L1, another predictive biomarker for cancer immunotherapy, $p = 0.31$) expression between the high- and low-risk groups (Fig. S5D). However, PD-1 ($p < 0.001$) and CTLA4 ($p < 0.001$) were obviously up-regulated in high-risk HCC patients (Figs. S5E–F).

4. Discussion

As the most common subtype in liver malignancy, HCC brings a great threat to human health all over the world along with a significant feature of increasing incidence and mortality. Although radical surgical resection can improve the OS, most HCC patients are diagnosed at an unresectable or advanced stage, accompanied by a poor outcomes of conventional radiotherapy and chemotherapy treatment [21]. Recently, immunotherapy, especially ICIs, has made great progress in the treatment of advanced HCC. However, the low response rate of ICIs limits the application of immunotherapy in the clinic, leading to an urgent need for effective predictive prognosis biomarkers for HCC patients. Pyroptosis, a novel type of programmed cell death, has been reported to be a double-edged sword for tumorgenesis and oncotherapy. Pyroptosis can transform normal cells into cancer cells by stimulating the release of inflammatory cytokines, while it can promote tumor cell death [[22, 23]], making pyroptosis a potential therapeutic and prognostic target for tumor. Considering that lncRNAs play important roles in various biological activities including cell pyroptosis in tumor, it is of great significant to identify a predictive pyroptosis-related lncRNA signature for improving the prognosis of HCC patients.

In this study, we constructed a prognostic risk signature comprising of 6 PRlncRs (MKLN1-AS, AC139491.2, AC145207.5, AC099850.3, AL590705.3 and AL049840.5) for predicting the OS, chemotherapeutic efficacy and ICIs response of HCC patients. Notably, among these 6 PRlncRs, MKLN1-AS has been reported to promote the proliferation, migration and invasion of HCC cells [24]. Based on 6 PRlncRs, we classified the HCC patients into high- and low-risk groups. The OS in low-risk group was significantly better than that in high-risk groups with a considerable accuracy (AUC = 0.762). We further created a predictive nomogram and found that the risk score was negatively related to clinicopathologic features including T stage, clinical stage and histological grade. The predictive ability of our risk signature was much better than other clinicopathologic features including age, gender, histological grade and clinical stage. The nomogram exactly forecasted the OS of patients and had excellent clinical utility.

Although chemotherapy is an important therapeutic modality for advanced HCC, it is usually of unsatisfactory efficacy and poor prognosis of HCC patients. In our study, it is available to predict the efficacy of Axitinib and Sorafenib for HCC patients base on the 6 PRlncRs risk signature, which could be used as a potential indicator of drug sensitivity. Given that pyroptosis, which has been reported to function in tumor immune microenvironment and immune infiltration, plays an important role in the OS in tumor patients, we revealed that the infiltration levels of $CD8^+$ T cells, memory activated $CD4^+$ T cells, follicular helper T cells, M1 macrophages cells decreased with the increase of risk score, in alignment with the reduced OS in high-risk HCC patients. In addition, the risk score was positively associated with the immune infiltration level of monocytes, M2 macrophages cells, eosinophils and neutrophils. Moreover, the immune-related signal pathways such as APC costimulation, CCR, checkpoint, HLA, MHC class I, parainflammation, T cell coinhibition and T cell costimulation pathways, were significantly enriched in high-risk HCC patients, which is associated with poor prognosis. According with the role of M2 macrophages promotes tumor progression, metastasis and chemotherapy resistance [[25–27]], HCC patients with abundance of M2 macrophages showed a reduced OS. In contrast, we found that high density of $CD8^+$ T cells could prolong the

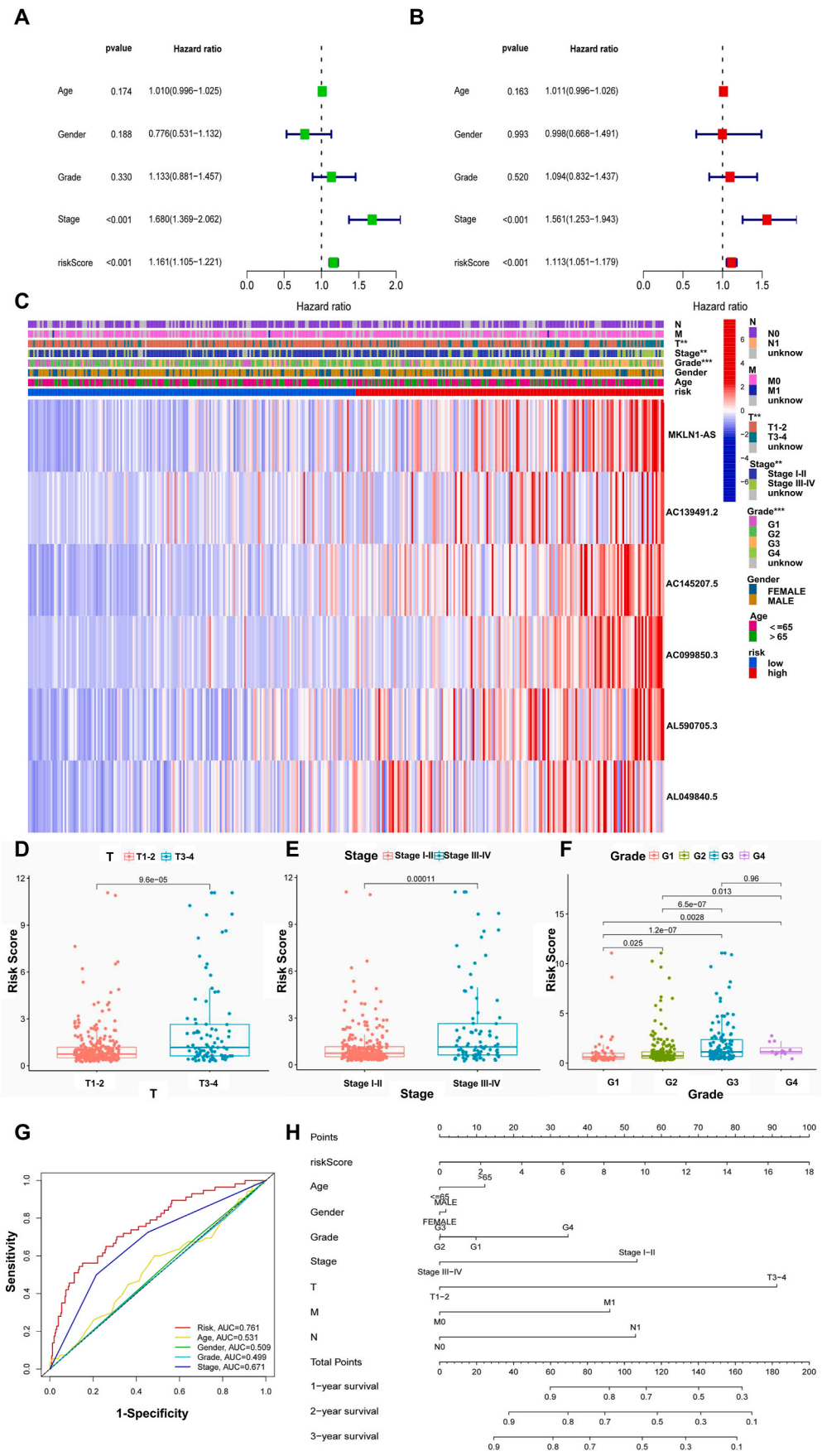

Fig. 3. Construction of a predictive nomogram. Hazard ratio of clinicopathologic characteristics and risk score in HCC analyzed by (**A**) Univariate and (**B**) multivariate Cox regression methods. (**C**) Heat map of clinicopathologic characteristics between high- and low-risk HCC patients. (**D-F**) The subgroup comparison of risk scores in different T stage (T1-2 and T3-4) (**D**), clinical stage (stage I-II and stage III-IV) (**E**) and histological grade (G1, G2, G3 and G4) (**F**). (**G**) ROC curves of measuring the predictive values of risk score, age, gender, grade and stage. (**H**) OS rates at 1-, 2- and 3-year of HCC patients predicted by constructed nomogram.

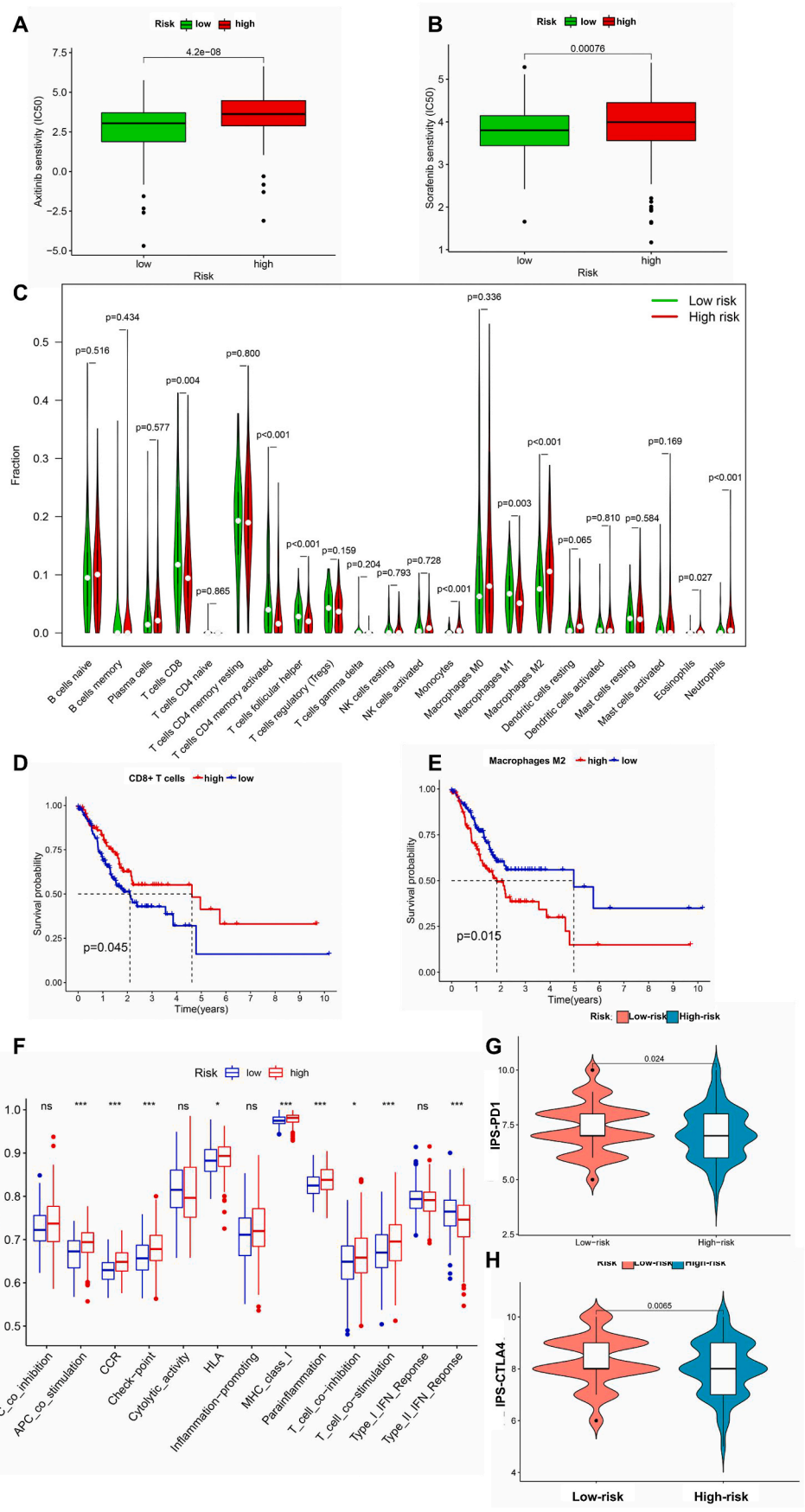

Fig. 4. Analysis of chemosensitivity, immune infiltration and ICI treatment predication between high- and low-risk HCC patients. (**A-B**) Half-maximal inhibitory concentration (IC50) of Axitinib (**A**) and Sorafenib (**B**) for HCC patients with high- and low-risk scores. (**C**) Comparison of 22 different immune cells in HCC. (**D**) OS curves for HCC patients with different infiltration levels of $CD8^+$ T cells. (**E**) OS curves for HCC patients with different infiltration levels of M2 macrophages. (**F**) Comparison of 13 different immune signal pathways in HCC. (**G-H**) IPS scores of PD1 (**G**) and CTLA4 (**H**) in high- and low-risk HCC groups.

OS in patients with HCC, which was consistent with recent observations that $CD8^+$ T cells in tumor antigen recognition and clinical responses [[28,29]]. Additionally, $CD8^+$ T cells are the effectors of ICI. The higher levels of $CD8^+$ T cell infiltration in tumors before and during ICI treatment, the more improved ICI efficacy [30], hinting that low-risk HCC patients with abundance of $CD8^+$ T cells, might benefit from ICI.

To date, despite $CD8^+$ T cells, several promising biomarkers for ICI response have been identified, including TBM, MSI and PD-L1 expression levels. Although the levels of TMB in high- and low-risk groups were similar, the risk score was negatively related to MSI. Due to the lack of ICI efficacy of HCC patients, we accessed IPS scores to determine the correlation between our risk signature and ICI treatment. HCC patients in low-risk group showed higher IPS scores of PD-1 and CTLA4 than those in high-risk group, proving again that low-risk HCC patients might benefit from ICI treatment. However, the expression levels of PD-L1, PD-1 and CTLA4 in HCC patients with low-risk scores were unchanged or even decreased. Although the status of these immune checkpoints above are recognized as predictive markers of immunotherapy [31], it needs to take into account about the use of immune checkpoints expression as a biomarker of eligibility for ICIs. For example, patients treated with ICI showed a better OS regardless of the PD-L1 status [32] and atezolizumab plus bevacizumab was approved by the FDA for patients with unresectable or metastatic HCC who had not received prior systemic therapy, irrespective of PD-L1 status [33]. Considering the effects of intratumoural heterogeneity and dynamic host immunity, further studies are needed to explore the relevance between the immune checkpoint status and the efficacy of ICI treatment for HCC patients.

Collectively, our study proposed a novel PRlncR prognostic model through comprehensive bioinformatics analysis, offering effective biomarkers to predict the OS, chemotherapeutic drug efficacy and ICI response for HCC patients. However, sufficient experimental verification is currently lacking in our study. Further studies should be carried out to explore the specific functions and regulatory mechanisms of 6 PRlncRs in HCC progression and immunotherapy.

Funding

This research was supported by the NSFC(31800684, 12172243), Postdoctoral Research Foundation of China (2021M703206), Natural Science Foundation of Shanxi Province (201801D221281).

Declaration of competinginterest

The authors declare that they have no known competing financial interests or personal relationships that could have appeared to influence the work reported in this paper.

Data availability

Data will be made available on request.

Appendix A. Supplementary data

Supplementary data to this article can be found online at https://doi.org/10.1016/j.bbrep.2022.101389.

References

[1] A. Forner, M. Reig, J. Bruix, Hepatocellular carcinoma, Lancet 391 (2018) 1301–1314.
[2] M.C. Wallace, D. Preen, G.P. Jeffrey, et al., The evolving epidemiology of hepatocellular carcinoma: a global perspective, Expet Rev. Gastroenterol. Hepatol. 9 (2015) 765–779.
[3] Y. Zongyi, L. Xiaowu, Immunotherapy for hepatocellular carcinoma, Cancer Lett. 470 (2020) 8–17.
[4] X. Li, C. Shao, Y. Shi, et al., Lessons learned from the blockade of immune checkpoints in cancer immunotherapy, J. Hematol. Oncol. 11 (2018) 31.
[5] K.S. Schneider, C.J. Groß, R.F. Dreier, et al., The inflammasome drives GSDMD-independent secondary pyroptosis and IL-1 release in the absence of caspase-1 protease activity, Cell Rep. 21 (2017) 3846–3859.
[6] Y. Wang, W. Gao, X. Shi, et al., Chemotherapy drugs induce pyroptosis through caspase-3 cleavage of a gasdermin, Nature 547 (2017) 99–103.
[7] L. Wang, K. Li, X. Lin, et al., Metformin induces human esophageal carcinoma cell pyroptosis by targeting the miR-497/PELP1 axis, Cancer Lett. 450 (2019) 22–31.
[8] E. Yue, G. Tuguzbaeva, X. Chen, et al., Anthocyanin is involved in the activation of pyroptosis in oral squamous cell carcinoma, Phytomedicine 56 (2019) 286–294.
[9] N. Pizato, B.C. Luzete, L. Kiffer, et al., Omega-3 docosahexaenoic acid induces pyroptosis cell death in triple-negative breast cancer cells, Sci. Rep. 8 (2018) 1952.
[10] D.C. Johnson, C.Y. Taabazuing, M.C. Okondo, et al., DPP8/DPP9 inhibitor-induced pyroptosis for treatment of acute myeloid leukemia, Nat. Med. 24 (2018) 1151–1156.
[11] J.E. Wilusz, H. Sunwoo, D.L. Spector, Long noncoding RNAs: functional surprises from the RNA world, Genes Dev. 23 (2009) 1494–1504.
[12] W.X. Peng, P. Koirala, Y.Y. Mo, LncRNA-mediated regulation of cell signaling in cancer, Oncogene 36 (2017) 5661–5667.
[13] Y.Y. Wang, X.L. Liu, R. Zhao, Induction of pyroptosis and its implications in cancer management, Front. Oncol. 9 (2019) 971.
[14] J. Feng, G. Yang, Y. Liu, et al., LncRNA PCNAP1 modulates hepatitis B virus replication and enhances tumor growth of liver cancer, Theranostics 9 (2019) 5227–5245.
[15] H. Wang, X. Huo, X.R. Yang, et al., STAT3-mediated upregulation of lncRNA HOXD-AS1 as a ceRNA facilitates liver cancer metastasis by regulating SOX4, Mol. Cancer 16 (2017) 136.
[16] J. Song, Y. Sun, H. Cao, et al., A novel pyroptosis-related lncRNA signature for prognostic prediction in patients with lung adenocarcinoma, Bioengineered 12 (2021) 5932–5949.
[17] W. Lin, Y. Chen, B. Wu, et al., Identification of the pyroptosis-related prognostic gene signature and the associated regulation axis in lung adenocarcinoma, Cell death discovery 7 (2021) 161.
[18] J. Jie, X. Xu, W. Li, et al., Regulation of apoptosis and inflammatory response in interleukin-1β-induced nucleus pulposus cells by miR-125b-5p via targeting TRIAP1, Biochem. Genet. 59 (2021) 475–490.
[19] Y. Ye, Q. Dai, H. Qi, A novel defined pyroptosis-related gene signature for predicting the prognosis of ovarian cancer, Cell death discovery 7 (2021) 71.
[20] L. Chang, M. Chang, H.M. Chang, et al., Microsatellite instability: a predictive biomarker for cancer immunotherapy, Appl. Immunohistochem. Mol. Morphol. : Appl. Immunohistochem. Mol. Morphol. AIMM 26 (2018) e15–e21.
[21] A.B. Benson, M.I. D'Angelica, D.E. Abbott, et al., Hepatobiliary cancers, version 2.2021, NCCN clinical practice guidelines in oncology, J. Natl. Compr. Cancer Netw. : J. Natl. Compr. Cancer Netw. 19 (2021) 541–565.
[22] R. Karki, T.D. Kanneganti, Diverging inflammasome signals in tumorigenesis and potential targeting, Nat. Rev. Cancer 19 (2019) 197–214.
[23] J. Ruan, S. Wang, J. Wang, Mechanism and regulation of pyroptosis-mediated in cancer cell death, Chem. Biol. Interact. 323 (2020), 109052.
[24] W. Gao, X. Chen, W. Chi, et al., Long non-coding RNA MKLN1-AS aggravates hepatocellular carcinoma progression by functioning as a molecular sponge for miR-654-3p, thereby promoting hepatoma-derived growth factor expression, Int. J. Mol. Med. 46 (2020) 1743–1754.
[25] D. Tu, J. Dou, M. Wang, et al., M2 macrophages contribute to cell proliferation and migration of breast cancer, Cell Biol. Int. 45 (2021) 831–838.
[26] Y. Chen, S. Zhang, Q. Wang, et al., Tumor-recruited M2 macrophages promote gastric and breast cancer metastasis via M2 macrophage-secreted CHI3L1 protein, J. Hematol. Oncol. 10 (2017) 36.
[27] M. Genin, F. Clement, A. Fattaccioli, et al., M1 and M2 macrophages derived from THP-1 cells differentially modulate the response of cancer cells to etoposide, BMC Cancer 15 (2015) 577.
[28] D.M. Pardoll, The blockade of immune checkpoints in cancer immunotherapy, Nat. Rev. Cancer 12 (2012) 252–264.
[29] P.C. Tumeh, C.L. Harview, J.H. Yearley, et al., PD-1 blockade induces responses by inhibiting adaptive immune resistance, Nature 515 (2014) 568–571.
[30] M. Sade-Feldman, K. Yizhak, S.L. Bjorgaard, et al., Defining T cell states associated with response to checkpoint immunotherapy in melanoma, Cell 175 (2018) 998–1013, e20.
[31] M. Reck, D. Rodríguez-Abreu, A.G. Robinson, et al., Pembrolizumab versus chemotherapy for PD-L1-positive non-small-cell lung cancer, N. Engl. J. Med. 375 (2016) 1823–1833.
[32] B.I. Rini, E.R. Plimack, V. Stus, et al., Pembrolizumab plus Axitinib versus sunitinib for advanced renal-cell carcinoma, N. Engl. J. Med. 380 (2019) 1116–1127.
[33] FDA Approves Atezolizumab Plus Bevacizumab for Unresectable Hepatocellular Carcinoma, Food and Drug Administration, 2020. https://www.fda.gov/drugs/resources-information-approved-drugs/fda-approves-atezolizumab-plus-bevacizumab-unresectable-hepatocellular-carcinoma. (Accessed 1 June 2020).